*29th EPS Conference on Plasma Phys. and Contr. Fusion Montreux, 17-21 June 2002 ECA Vol. **26B**, P-2.064 (2002)*

Transport studies in DIII-D with modulated ECH

J.C. DeBoo,[1] M.E. Austin,[2] R.V. Bravenec,[2] J.E. Kinsey,[3] J. Lohr,[1] T.C. Luce,[1] G.R. McKee,[4] C.C. Petty[1], R. Prater,[1] T.L. Rhodes,[5] G.M. Staebler,[1] L. Zeng[5]

[1]*General Atomics, P.O. Box 85608, San Diego, California 92186-5608 USA*
[2]*Fusion Research Center, The University of Texas, Austin, Texas USA*
[3]*Lehigh University, Bethlehem, Pennsylvania 18015 USA*
[4]*University of Wisconsin, Madison, Wisconsin 53706-1687 USA*
[5]*University of California, Los Angeles, Box 951597, Los Angeles, California 90095 USA*

ABSTRACT

Experiments have been performed where the T_e profile stiffness was tested at several spatial locations by varying the ECH resonance location. Propagation of the pulses was Fourier analyzed and compared to simulations based on several transport models. The plasma appears to be near the critical T_e gradient for ETG modes and marginally stable to ITG modes. However, the local T_e response to a locally applied heat pulse does not indicate a nonlinear, critical gradient model where T_e is clipped when trying to rise above a critical gradient. The response can be simply understood as the plasma integrating the ECH power, producing an increase in T_e which equilibrates to a new local level with an exponential time constant representing the local confinement time.

TEST OF T_e PROFILE STIFFNESS

Measuring the plasma response to local heat pulses produced by electron cyclotron heating (ECH) has been shown to be a sensitive test of plasma transport properties and provides a means to critically test transport models of both electron and ion behavior [1]. Recent experiments in ASDEX-Upgrade have shown that a simple model for the electron thermal diffusivity based on a critical temperature gradient can reproduce the stiff T_e profiles observed in L-mode and H–mode plasmas [2]. Results from modulated ECH experiments in DIII-D are reported here for L-mode plasmas where neutral beam heating was dominant.

The experiments were carried out in elongated, κ=1.5, L-mode plasmas limited against the inside wall of the vessel in order to avoid H-mode. During the current ramp up to 0.8 MA, 4 MW of NB power was applied in order to slow down current penetration and delay the onset of sawteeth. During the sawtooth-free, current flattop period from 1 to 2 s, 1 MW of ECH power modulated at 25 Hz was applied. The ECH resonance location was varied at fixed toroidal field, B_T=2.0 T, by varying the poloidal angle of the launch antenna. The temperature profile was probed shot by shot at four locations, ρ_{ECH} = 0.2, 0.4, 0.6 and 0.7. The temperature, density, rotation, and Z_{eff} profiles in each of these four cases were very similar as shown in Fig. 1. Note that $T_i/T_e \sim 1$ over the mid-region of the plasma.

The fractional change in T_e was approximately 10% for all four cases. The magnitude of the change in local T_e can be seen in Fig. 2. A 40 ms (the modulation period) moving average was subtracted from the raw electron cyclotron emission signal, 20 pulses were then averaged. Note that the shape of the T_e pulse produced becomes more square like toward the edge of the plasma. The pulse shape at ρ = 0.7 could indicate a stiff profile response where a critical T_e gradient had been exceeded leading to an abrupt halt to the rise in T_e. The dashed lines in Fig. 2 will be discussed later.

Power balance analysis of these discharges indicates that the T_e profile may be at a critical gradient or critical gradient scale length. Figure 3(a) displays the electron thermal diffusivity, χ_e, versus a normalized gradient scale length R/L_{Te}. For each case there is a large

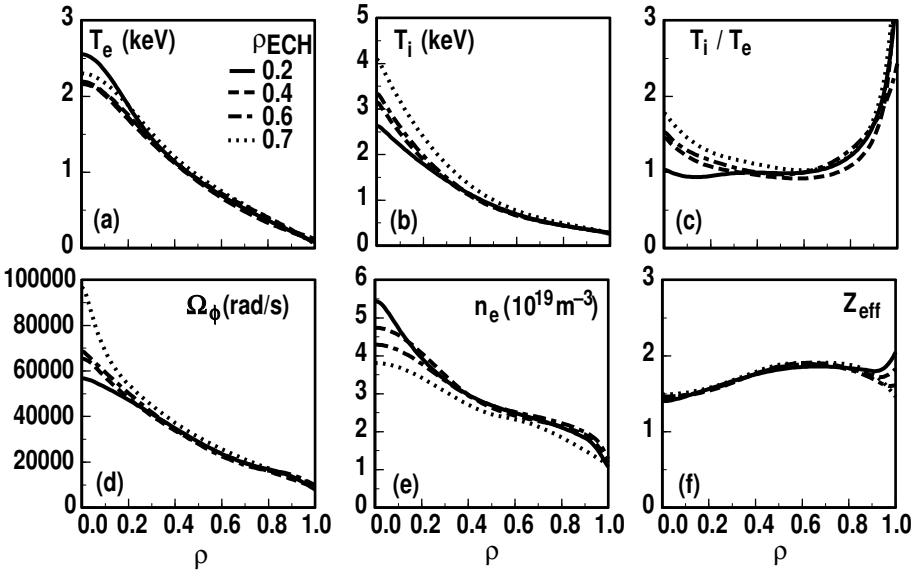

Fig. 1. Spatial profiles of (a) electron temperature, (b) ion temperature, (c) T_i/T_e ratio, (d) toroidal rotation velocity, (e) electron density and (f) effective charge for the four cases with ECH resonant at ρ_{ECH} = 0.2, 0.4, 0.6 and 0.7.

change in χ_e at R/L_{Te} ~ 5. Figure 3(b) indicates that this value exists over a large portion of the plasma, ρ ~ 0.2–0.7. This is the same region of the plasma, however, where the response to a local heat pulse (Fig. 2) does not indicate a stiff response (with the possible exception of the case at ρ_{ECH} = 0.7). If R/L_{Te} ~ 5 is a critical value, then operation at this value does not imply a stiff temperature profile.

Critical gradients from drift wave stability calculations with the GKS code [3] indicate that the plasma is at the marginality condition for both electron and ion temperature gradient, ETG and ITG, modes over most of the plasma. The critical gradient for ETG modes is R/L_{Te} ~ 5 for ρ = 0.2–0.8 the same value shown in Fig. 3(b) for the plasma for ρ = 0.3–0.7. At larger radii the measured values of ∇T_e are above the ETG mode critical gradient. The maximum growth rate for ITG modes is fairly small, γ_{max} ~ 5×10^4 s^{-1}, and is comparable to the stabilizing E×B flow shear rate in the region ρ = 0.2–0.6. Toward the edge, trapped electron modes dominate the unstable growth rates. Further evidence of drift wave activity exists from low-k density fluctuation measurements near the plasma edge. Amplitude modulation of low-k turbulence was observed just inside the ECH resonance location, and out of phase with respect to the ECH pulses [4].

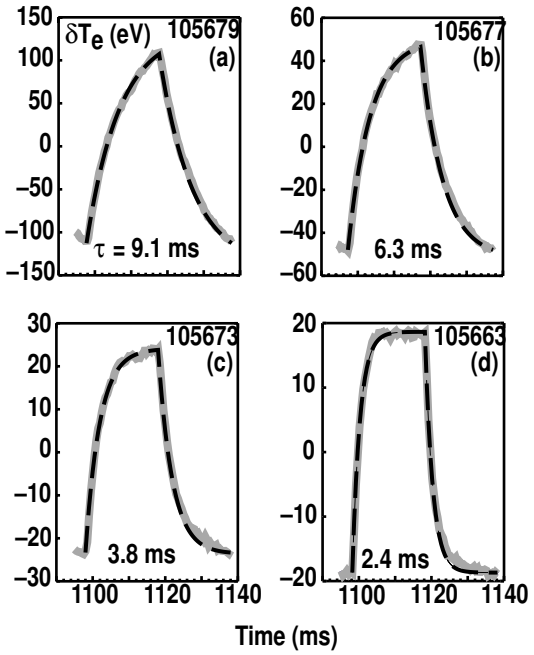

Fig. 2. Local change in electron temperature at the ECH resonance locations (a) ρ_{ECH} = 0.2, (b) ρ_{ECH} = 0.4, (c) ρ_{ECH} = 0.6 and (d) ρ_{ECH} = 0.7 (shown in gray). Dashed lines represent a fit of the rise of each pulse proportional to $(1–e^{t/\tau})$ where the fit constant τ represents the local confinement time.

The T_e response does not require the existence of a critical temperature gradient, even for the case at $\rho_{ECH} = 0.7$. The local T_e response can be modeled as a rise in T_e that asymptotes in time as $(1-e^{t/\tau})$ with time constant τ. The dashed lines in Fig. 2 are the result of such a fit to the rise time of each of the pulses. The decrease in T_e represented by the dashed curves is described by the same time constant as the rise time and shows that the process is reversible. The time constant τ, which can be interpreted as the local confinement time, is given in Fig. 2 and shows that the local confinement time decreases toward the plasma edge. For $\rho_{ECH} = 0.7$ the local confinement time (2.4 ms), becomes small compared to the 20 ms duration of the heating pulse. Under this condition a new equilibrium temperature is established and maintained during the heating pulse as is shown in Fig. 2. Thus even this apparently stiff looking response does not require one to invoke a nonlinear, critical gradient process. One additional experiment was performed with 4 gyrotrons with $\rho_{ECH} = 0.76$, about twice the power of the cases shown in Fig. 2, and resulted in $\delta T_e \sim 60$ eV and a slightly lower local confinement time, 1.7 ms, consistent with being closer to the plasma edge. More importantly this case indicated that further increases in δT_e were possible near the plasma edge without showing signs of nonlinear clipping.

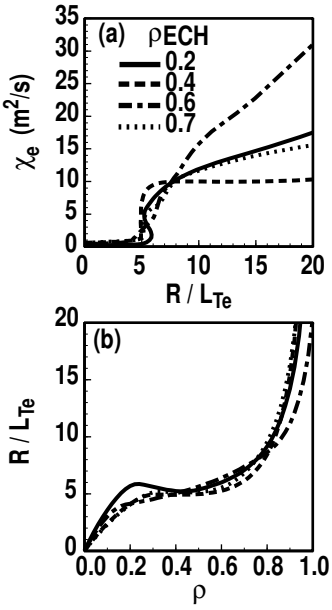

Fig. 3. (a) Electron thermal diffusivity versus normalized temperature gradient scale length, R/L_{Te}, and (b) spatial profile of R/L_{Te}.

TEST OF TRANSPORT MODELS

Fourier analysis of heat pulse propagation from the plasma edge toward the center was compared to simulations from three transport models, a renormalized GLF23 model [5], the Multimode (MM) model [6], and the IFS/PPPL model [7]. Renormalization of the GLF23 model decreased the ITG/TEM transport levels while increasing the ETG transport level. The multimode, MM, model was run without kinetic or resistive ballooning modes and with enhanced electron neoclassical diffusivity, equal to ion neoclassical values. The IFS/PPPL and GLF23 models were run including E×B shear effects. Only the GLF23 model was run with momentum transported. For the other two model simulations the measured toroidal velocity profiles were held fixed.

Heat pulse propagation studies allow a critical test of transport models since both the dynamic and equilibrium properties of the models can be tested. Figure 4 displays a comparison of the model simulations and experimental data, for modulated (Fourier phase and amplitude of the fundamental frequency) and equilibrium temperature profiles for both electrons and ions. The data shown is for a discharge with $\rho_{ECH} = 0.76$ and twice the ECH power discussed earlier, which made observation of the ion response more clear. Both the MM and GLF23 models match the equilibrium T_e profile reasonably well. Only the GLF23 model matches the Fourier phase of the electrons well while none of the models matches the electron Fourier amplitude very well. The simulations of the dynamic response of the ions is rather similar for all three models however the MM model matches the ion equilibrium temperature somewhat better than the other two models. Overall, no single model compares

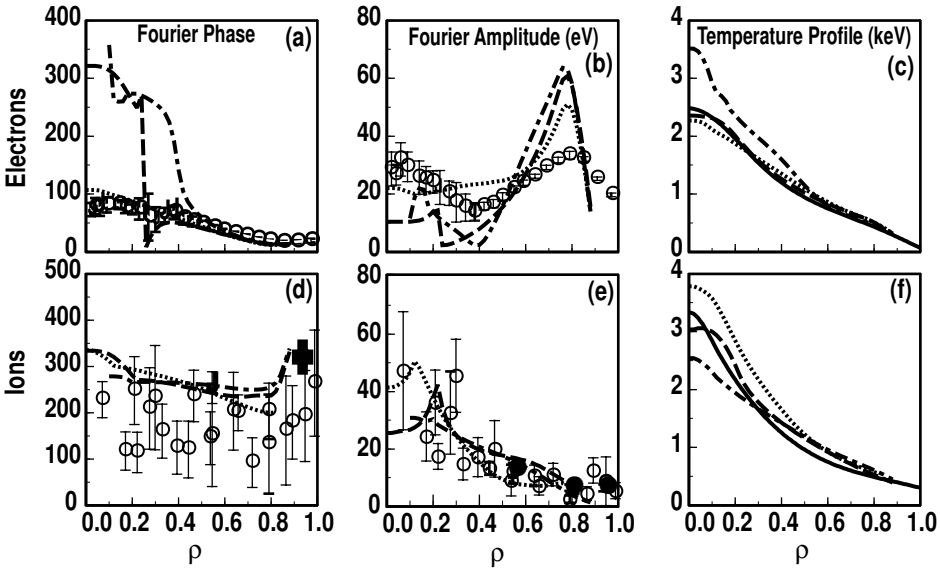

Fig. 4. Fourier analysis of δT_e and δT_i for phase and amplitude at fundamental frequency 25 Hz and T_e and T_i for experimental data (circles and solid black lines), renormalized GLF23 model (dotted lines), the Multimode model (dashed lines) and IFS/PPPL model (chain dashed lines) for a case with $\rho_{ECH} = 0.76$.

well with both the electron and ion responses. The GLF23 model provides the best match to the electrons while the MM model is somewhat better for the ions.

It is worth noting that the considerable increase in electron phase as the heat pulse propagates away from the deposition region, see Fig. 4, is a further indication that the T_e profile is not very stiff. A stiff response would be indicated by a very small change in phase as the pulse propagated toward the center of the discharge. Finally, it is interesting to note the rise in the measured electron Fourier amplitude for $\rho < 0.35$ in Fig. 4. This phenomena is not expected for a simple diffusive process, but is produced by some as yet unidentified mechanism. Further study of the IFS/PPPL model may help in understanding the phenomena as the trend in this model has similar behavior.

ACKNOWLEDGMENT

Work supported by U.S. Department of Energy under Contract DE-AC03-99ER54463, and Grants DE-FG03-97ER54415, DE-FG02-92ER54141, DE-FG03-96ER54373, and DE-FG03-01ER54615.

REFERENCES

[1] DeBoo, J.C., et al., NF **39** (1999) 1935.

[2] Ryter, F., et al., Phys. Rev. Lett. **86** (2001) 2325 and 5498.

[3] Waltz, R.E. and Miller, R.L., Phys. Plasmas **6** (1999) 4265 and Kotschenreuther, M. et al., Comput. Phys. Commun. **88** (1995) 128.

[4] R.V. Bravenec, et al., Poster P-2.067, this conference.

[5] Kinsey, J.E., et al., 3B3 in Proceedings of 2002 International Sherwood Fusion Theory Meeting, 2002 and Waltz, R.E., et al., Phys. Plasmas **4** (1997) 2482.

[6] Kinsey, J.E., et al., Phys. Plasmas **3** (1996) 3344.

[7] Kotschenreuther, M., et al., Phys. Plasmas **2** (1995) 2381.